Effect of NAPL mixture and alteration on 222Rn partitioning coefficients: Implications for NAPL subsurface contamination quantification

Mathieu Le Meur, Grégory J.V. Cohen, Mélissa Laurent, Patrick Höhener, Olivier Atteia

Effect of NAPL mixture and alteration on ^{222}Rn partitioning coefficients: implications for NAPL subsurface contamination quantification

Le Meur Mathieu[a], Cohen Grégory J. V.[a], Laurent Mélissa[a], Höhener Patrick[b], Atteia Olivier[a]

[a] EA 4592 G&E, Bordeaux INP - Université Bordeaux Montaigne - Carnot ISIFoR, 1 allée F. Daguin, 33607 Pessac, France

[b]Aix-Marseille Université - CNRS, Laboratoire Chimie Environnement UMR 7376, 3 place Victor Hugo, 13331 Marseille, France

Abstract

Soils and groundwater are often contaminated by complex organic mixtures also called Non Aqueous Phase Liquids (NAPLs). Several techniques such as drilling, monitoring of soil gas or injection of tracers are traditionally used to quantify NAPLs in aquifers but are complex to perform. The use of natural soil gas such as ^{222}Rn could be an easy and cheap alternative. This method requires the knowledge of the radon NAPL-water partitioning coefficients ($K_{n\text{-}w}$.). Once spilled on soil, NAPL will undergo degradation (evaporation, effects of sun light among others) and this degradation could impact the $K_{n\text{-}w}$. This study aims at investigating the partitioning coefficients of complex NAPLs such as commercial diesel fuel and gasoline in relation to degradation such as evaporation and UV-degradation. For that purpose, batch experiments and GCMS investigations were carried out. The results show different $K_{n\text{-}w}$ for the commercial diesel fuel (60.7 ± 6.1) and gasoline (37.4 ± 5.6) The results also show different $K_{n\text{-}w}$ behaviors in relation with degradation. Degraded diesel fuel display opposite $K_{n\text{-}w}$ values (74.8 ± 7.5 and 25.1 ± 2.5 for UV degraded and evaporated diesel fuel, respectively), compared to fresh one. Degraded gasoline shows no significant variations of the $K_{n\text{-}w}$ compared to fresh one. The molecular investigation reveals the removal of the most volatile fraction for the evaporation treatment, whereas

UV-degradation do not have pronounced effects on the chromatogram pattern. For the gasoline molecular investigation, no difference is observed between the treatments excepted a very slight removal of the lightest compounds under evaporation. These results show that NAPL degradation have effects on the K_{n-w} for diesel fuel and no significant effects for gasoline, at least with these degradation paths. This K_{n-w} variation will have *in fine* effects on ^{222}Rn activity interpretation and NAPL subsurface quantification.

Key words: ^{222}Rn, Fresh and altered NAPL, Radon Partitioning Coefficient, NAPL Subsurface Contamination quantification

Highlights

- Radon partitioning coefficients were determined for fresh and altered NAPLs
- Molecular signatures of fresh and altered NAPL were investigated using GC-MS
- Altered and fresh diesel fuel showed different NAPL-water partitioning coefficients
- Altered and fresh gasoline showed similar NAPL-water partitioning coefficients
- The partition coefficient is of pivotal importance for NAPL delineation

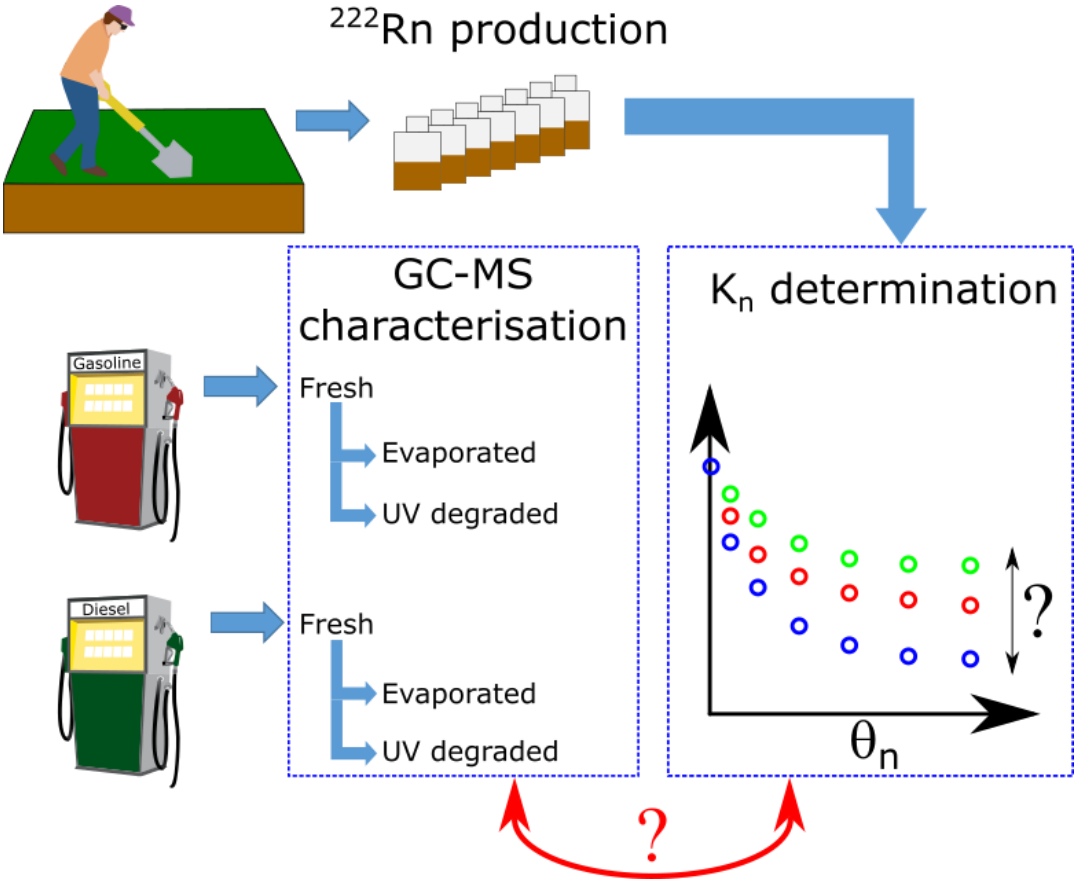

1. Introduction

Soil and groundwater are often contaminated by complex organic mixtures, such as petroleum products or chlorinated solvents (also known as Non-Aqueous Phase Liquids, or NAPL), and these liquids are recognized as a critical issue in environmental remediation (Davis et al., 2003). These NAPL are frequently encountered in industrial or military sites and are releasing toxic compounds to groundwater. They can persist sometimes for centuries, creating long-term contamination due to their low solubility in water (Cohen and Mercer, 1993; Zhang et al., 1998). NAPL can be released to the environment during fueling, maintenance and/or storage operations. Large volume of spilled NAPL can migrate through unsaturated soil zone to the water table (Yoon et al., 2013). This migration is complex, following preferential pathways and forming ganglia and small isolated lenses (Fernandez et al., 2013). The light NAPLs preferentially float at the top of the water table and dense NAPLs penetrate into the saturated zone (Castelluccio et al., 2018). During the migration through the vadose zone, a certain amount of liquid (up to 20%, known as residual saturation) is retained in the pores by capillary forces forming a source zone (Wiedemeier et al., 1999) where gaseous and aqueous contaminant plumes are formed (Höhener and Surbeck, 2004). It is then crucial to accurately detect, localize and quantify residual NAPL sources prior to choose efficient remediation procedures.

Traditionally, soil NAPL contamination has been estimated using sampling techniques (drilling and core-sampling) which are of very high quality but are expensive and time consuming (Feenstra and Cherry, 1996; Yoon et al., 2013). In addition, without prior information concerning the contamination pattern, the position of the sampling stations could lead to useless data (Garcia-Gonzalez et al., 2008). Screening method such as gas monitoring (in particular Volatile Organic Compounds, VOCs, Wilson et al. 1997) is another non expensive technique that permits to approximately locate the contamination source zone laterally and vertically (Robbins et al., 1990). However, NAPL degradation leads to high VOC concentrations that do

not reflect the amount of NAPL (Höhener and Surbeck, 2004) in the source zone. This last technique is thus only suitable for volatile contaminants and hence not suitable for diesel fuel, fuel, kerosene or hydraulic oil (Schubert et al., 2005). The injection of artificial tracers directly in soils is another technique cited in the literature (Deeds et al., 1999; Brusseau et al., 2003). The gas is directly injected in the vadose zone where it can be transported by advection (Mariner et al., 1999) and/or diffusion (Werner and Hohener, 2002) and the interpretation of the breakthrough curves permits to obtain the localization and the average volumetric NAPL content (Dwarakanath et al., 1999). However, this technique is time consuming, expensive (Höhener and Surbeck, 2004) and can give quite misleading results in heterogeneous environment (Nelson et al., 1999). Due to the limitations of the different techniques cited above, alternative options must be proposed. A simpler way to investigate subsurface contaminations is the use of native soil gas that partitions into NAPLs.

Radon-222 (^{222}Rn) is a good advocacy for the understanding of NAPL behavior in subsurface (Barrio-Parra et al. 2021). ^{222}Rn is a natural component, continuously produced in soil matrices by the alpha-particle decay of ^{226}Ra in the natural decay of the uranium-238 series (DeWayne-Cecil and Green, 1999). ^{222}Rn also decays by alpha-particle decay and has a half-life of 3.82 days (Mason and Moore, 1982). Uranium is ubiquitous in minerals, as a trace element, permitting almost ubiquity production of radon in the environment. The ^{222}Rn emanation coefficient corresponds to the gas fraction released from the host materials which is retained in the pore space (Andrews and Wood, 1972). The composition and mineralogy of the soil, and thus especially the particle size contribute to the emanation coefficient. In general, when the particle size is small, the specific surface area is large and the emanation power of materials containing ^{226}Ra is higher (Galhadi and Bonotto, 2012; Thu et al., 2020). Other chemical and physical parameters can also influence the radon activity such as moisture content and pore size (Nazaroff, 1992; Galhardi and Bonotto, 2012; Cujic et al., 2020).

96 The use of natural radon to localize and quantify NAPL amount in subsurface is feasible
97 because its preferential partition into organic phase (Horiuchi and Murakami, 1981; Hunkeler
98 et al., 1997; Nazaroff, 1992; Sakoda et al., 2011; Semprini et al. 2000; Wong et al., 1992). When
99 groundwater containing radon migrates towards a residual NAPL contamination area, a local
100 radon deficit in groundwater is then observed (Hunkeler et al., 1997; Schubert et al., 2007a).
101 The radon deficit close to a NAPL-contaminated zone depends on (i) the pore space saturated
102 with residual NAPL and (ii) the radon partitioning coefficient specific for the NAPL present
103 (Schubert et al., 2007a). If the ^{222}Rn partitioning coefficient of the NAPL is known, it is possible
104 to localize and quantify the residual saturation of the organic phase (Schubert et al., 2007a;
105 Cohen et al., 2019). The knowledge of the partitioning coefficient is therefore of pivotal
106 importance when dealing with site NAPL contamination delineation. Several partitioning
107 coefficients have been mainly reported for pure organic compounds (Clever, 1979, Schubert et
108 al., 2007b) but few authors reported the partitioning coefficient for commercial NAPL mixtures
109 (Schubert et al., 2002; 2007a). Schubert et al., (2007b) worked on the ^{222}Rn partitioning
110 between air, water and three artificial NAPL mixtures. They stated the need of experiments on
111 NAPL mixtures in order to verify or modify the theoretical framework. Schubert (2015) also
112 mentioned that NAPL degradation could affect its complex composition, leading in return to a
113 change of the partitioning coefficient. This change of the partitioning coefficient will affect the
114 NAPL quantification in soils. However, to our knowledge, no study in the literature deals with
115 the effect of NAPL alteration on ^{222}Rn partitioning coefficient.
116 When spilled on the soil, the NAPL will be exposed to wind and heat for a certain time which
117 might be sufficient to evaporate the light NAPL fraction (Villa et al., 2010). In soils, NAPL
118 may undergo biodegradation, governed by microorganisms, leading to the loss of contaminants
119 (Wiedmeier et al., 1999) and the modification of initial NAPL composition. Natural NAPL
120 biodegradation takes time and depends on different parameters such as soil properties (Jho et

al., 2014) and microorganism's ecology in action. These NAPL chemical alterations should thus lead to a ^{222}Rn partitioning coefficient modification.

In the frame of the above discussion, the objectives of this article are (i) to determine the partitioning coefficient of mixed commercial NAPLs, (ii) to investigate the effects of NAPL degradation on ^{222}Rn partitioning coefficient and (iii) to investigate the relationship between the partitioning coefficient modification and NAPL chemical composition. To reach these goals, batch experiments were conducted to determine ^{222}Rn soil production and water-NAPL partitioning coefficient ($K_{n\text{-}w}$) in fresh and degraded complex NAPL mixtures. These experiments aim at better characterizing the ability of ^{222}Rn method to delineate NAPL pollution at contaminated sites.

2. Material and methods

2.1. Porous media

The porous media used is this study is an alluvial sand from the Aquitaine basin (France). It was sampled in a natural soil and sieved in order to only retain the fine fraction (710 – 250 µm) which presents higher ^{222}Rn emanation coefficient (Chitra et al., 2018). The density of this soil fraction was measured using a pycnometer (Rodier et al., 2009).

2.2. Reagents

Six NAPLs were used in this study. Two of them are commercial "fresh" gasoline (SP98) and diesel fuel, both obtained from a pump at a road fuel station (Casino supermarket, France). Four were obtained from the degradation of both "fresh" NAPLs following two degradation paths (described below). For NAPLs dilution prior liquid GC-MS injections, n-heptane solvent (n-Heptane, 99+%, residues analysis, ACROS Organic, UK) was used.

2.3. NAPL characterization and degradation

2.3.1. NAPLs density

As for the porous media, NAPLs densities were characterized using a pycnometer (Rodier et al., 2009).

2.3.2. GC-MS analysis

In order to characterize chemical compositions of fresh and altered NAPLs, GC-MS analyses were conducted. These analyses were performed using two devices to increase the separation and thus identification ability of this study, the first and second one performing liquid and Head-Space (HS) injections, respectively. Indeed, HS-GC-MS technique permits the detection of the most volatile compounds, and has a low detection limit, suitable for diesel fuel compounds identification (D'Auria et al., 2008; Safarova et al., 2004). The liquid GC-MS is also suitable for NAPL investigation as they contain heavy hydrocarbons with long chain, easily detectable using this technique (D'Auria et al., 2008). For both analytical systems, ultra-high purity He (Alphagaz 2, Air Liquide, France) was used as carrier gas.

Liquid injections were performed on a GC (7820A, Agilent, USA) equipped with a low polarity HP-5ms (30 m × 250 µm × 0.25 µm, Agilent, USA) column and coupled with a mass spectrometer (5977E, Agilent, USA) operated with an electron ionization (EI) source. The GC operating parameters for the liquid injections were: splitless mode injection of 1 µl (NAPLs diluted at 2 mg. L^{-1}) at 280°C with a constant flow rate of 1 mL min^{-1}. The primary oven temperature was programmed at 50°C during 5 min then ramping at 5°C min^{-1} to 300°C and hold for 20 min.

Head-Space (HS) injections were performed on a GC (8860, Agilent, USA) equipped with an intermediate polarity Rxi-624 Sil MS (30 m x 250 µm x 1.4 µm, Restek, USA) column, which is more appropriate for volatile compounds separation, coupled to a mass spectrometer (5977B, Agilent, USA) containing a EI-Xtr source. The GC operating parameters for the HS injections were: split ratio (20:1) mode injection of 0.5 mL at 280°C with a constant flow rate of 1.5 mL min^{-1}. The primary oven temperature was 35°C during 1 min, then ramping at 5°C min^{-}

[1] to 300 °C and hold for 20 min. Prior HS injections, each vial was incubated at 60°C for 30 min and head-space phase sampled with a syringe heated at 60°C.

The MS parameters were the same for both devices: electron ionization mode with an electron energy of 70 eV. The ion source and quad temperatures were 230 and 150°C, respectively. MS acquisition was done in SCAN mode, analyzing m/z between 25 and 300 amu and included a 5 min solvent delay for liquid injections. Chromatograms were interpreted with Masshunter Qual software (Agilent, USA) and mass spectrum compared to the literature (Turner and Goodpaster, 2012; Naggar et al., 2017) and to the NIST MS 2.2 2017 database.

A semi-quantification was applied for the samples. The proportion of different families (linear-alkanes, ramified-alkanes, monoaromatics, cycloalkanes) was integrated. For that purpose, the proportion of each family (%) class was calculated by dividing the sum of the area of different compounds of each family by the sum of the peak areas of all analyzed compounds of fresh NAPL (TIC) and multiplied by 100.

2.3.3. Degradation of commercial NAPLs

As it is difficult to mimic natural biodegradation under laboratory conditions “fresh” NAPLs were artificially degraded using two different methods: evaporation and UV degradation.

Concerning the first one, a simple 50% and 30% weight evaporation of the gasoline and diesel fuel, respectively, was performed in order to remove the most volatile compounds. For that purpose, 700 g of fresh NAPLs were placed in a beaker (200 cm^2) and exposed at open air under the hood for two weeks and 2 hours for diesel fuel and gasoline, respectively. The photodegradation experiments were carried out in a photolytic reactor which consists in a 1 L glass bottle. A UV light (TUV PL-L 95w/4P HO, 250 nm, Philips) was placed close to the reactor and the set up was wrapped with aluminum foil to avoid radiation release. A mass of 350 g of fresh NAPL was inserted into the reactor and exposed under UV light for two hours at room temperature with magnetic stirring (110 rpm).

2.4. Batch experiments

In order to determine the evolution of ^{222}Rn partitioning coefficient between gas and NAPL, depending on NAPL chemical composition, eight sets of batch experiments were conducted in this study, each set performed with 6 (^{222}Rn production) or 6 ($K_{n\text{-}w}$ determination) batches presenting different fluids contents. The two first sets were dedicated to the measurement of the ^{222}Rn production of the porous media coming from the same area, but at different depths (20 and 70 cm) in order to investigate the ^{222}Rn production variability of a large volume of soil. The third and fourth sets of batch were dedicated to the determination of the partitioning coefficient of the fresh gasoline and diesel fuel (14 batches). The sets 5-8 permitted this characterization for artificially degraded commercial NAPL mixtures.

All the different sets of experiments were performed using 1 L glass bottles sealed with gas tight pre-perforated rubber stoppers as they prevent any gas linkage (Cohen et al., 2019). Gas leakage was checked for every batch by lowering the pressure in the batch and by monitoring the pressure during 5 min. Then, the atmospheric pressure was restored using a syringe needle. A mass m_s ($\sim$ 700g) of sieved soil was chosen for each batch. Different water and NAPL (if applicable) contents were chosen and mixed with the porous media prior insertion of the mixture in the batch. For batches with NAPL, prior NAPL contamination, the dry porous media was moistened with a desired volumetric water content (θ_w= 0.02) in order to better mimic natural conditions. For each set of batches containing the different NAPLs (fresh and degraded), one batch was dedicated to the measurement of the ^{222}Rn activity without NAPL at a water content similar to the batches with NAPL (θ_w=0.02), referred hereafter as “check-batches”. These check-batches were used in order to verify the ^{222}Rn production for the amount of soil used for each set of batches. The batch reactors were left for 25-30 days to reach radioactive equilibrium before ^{222}Rn activity measurement (Höhener and Surbeck, 2004).

2.5. ^{222}Rn activity measurements

Scintillation flasks of 125 cm^3 (Algade, France) were used for ^{222}Rn measurements. First, a pump (Neuberger 816, KNF, Germany) was used to vacuum the flasks (-850 to -900 mbar). Then, the soil-gas from the batch was extracted by suction, using a steel needle linked to a valve. The flasks were inserted into the counter chamber of a portable alpha counter (CAPP2, Algade France) and kept in the dark for 10 min. After radioactive equilibrium, ^{222}Rn activity in each flask was determined six times with counting times of 20 min. Radon background, referred as blank values was measured on the same flask, under the same counting conditions and were subtracted. The yields of each flask were taken into account and the radon activity expressed in Bq m^{-3} was obtained using previously established calibration. The ^{222}Rn production (Bq kg^{-1}) was then calculated (equation 1) taking into account the batch properties (mass of soil, water and gas contents):

Eq. (1) $$A = \frac{1}{\left(1+\frac{\theta_w}{K_H\theta_g}+\frac{K_n\theta_n}{\theta_g}\right)}\frac{m_s}{V_g}EC_{Ra}$$

With A the ^{222}Rn activity ($Bq.m^{-3}$), θ_w the water content (-), K_H the gas–water partitioning coefficient (-), θ_g the gas content (-), K_n the NAPL-gas coefficient (-), θ_n the NAPL content, m_s the mass of soil (kg), V_g the volume of gas (m^3), E the ^{222}Rn emanation coefficient (-) and C_{Ra} the solid ^{226}Ra content (Bq kg^{-1}). The NAPL-water partitioning coefficient was also calculated:

Eq. (2) $K_{n\text{-}w} = K_n \times K_H$

In order to test the effect of $K_{n\text{-}w}$ modification on NAPL saturation (S_n), the equation presented in Hunkeler et al. (1997) was used:

Eq. (3) $S_n = (Ae^{napl=0}/Ae^{napl>0}\text{-}1)/(K_{n\text{-}w}\text{-}1)$

242 With S_n the NAPL saturation (-), $Ae^{napl=0}$ the ^{222}Rn activity in the batches without NAPL

243 ($Bq.m^{-3}$), $Ae^{napl>0}$ the ^{222}Rn activity in the batches with NAPL ($Bq.m^{-3}$) and K_{n-w} the NAPL

244 water partition of ^{222}Rn (-).

3. Results

3.1. Porous media and NAPLs densities

The density of the PM is 2631 ± 4.2 kg.m^{-3}. Concerning NAPLs, fresh, UV-degraded and evaporated diesel fuel densities are about 813 ± 3.8, 812 ± 3.8 and 843 ± 3.8 kg m^{-3}, respectively, while they are about 748 ± 3.8, 746 ± 3.8 and 796 ± 3.8 kg m^{-3} for fresh, UV-degraded and evaporated gasoline, respectively. Thus, significant density differences can be observed for NAPL evaporation with an increase of about 4 and 6% for diesel fuel and gasoline, respectively.

3.2. ^{222}Rn production of Porous media

The results concerning the soil ^{222}Rn production (EC_{Ra}) in the different batches are presented in Fig. 1. The results are presented in function of the batches water content (θ_w). For the 20 cm depth soil, EC_{Ra} increases rapidly from 1.49 ± 0.25 Bq kg^{-1} (dry sample) to 2.65 ± 0.25 Bq kg^{-1} (θ_w 0.02). Then, the EC_{Ra} decreases and remain relatively constant (mean of 2.49 ± 0.13 Bq kg^{-1}) for larger water contents (θ_w 0.04 – 0.1). Concerning the 70 cm depth soil, the production follows the same behavior but presents lower values, with for the dry sample, an EC_{Ra} value of 0.95 ± 0.25 Bq kg^{-1} which increases to 1.33 ± 0.32 Bq kg^{-1} (θ_w 0.1) with a mean of 1.29 ± 0.34 Bq kg^{-1}. The ^{222}Rn activities measured in the production batch with a water content of θ_w = 0.02 are 2090 ± 264 Bq m^{-3} at 20 cm and 1005 ± 268 Bq kg^{-1} at 70 cm. In addition, the ^{222}Rn production measured in the "check-batches" (7 batches coming from the different sets) are comprised between 1.3 and 2.5 Bq kg^{-1} for the two sets of batches with different soils depth (Fig. 1). Since the production for the "checked batches" is in the range of the production batches, for each set of batch, the "checked batch" corresponding production was chosen instead of the mean production (Fig. 1) due to the ^{222}Rn production variation.

3.3. NAPL-gas partitioning coefficient (K_n) of ^{222}Rn for fresh and altered diesel fuel and gasoline

3.3.1. Partitioning coefficient (K_n) of fresh and altered diesel fuel

The ^{222}Rn activities in the batches containing fresh diesel fuel at different volumetric contents are presented in Figure 2a. The Supplementary Information (SI) presents the statistical results permitting to conclude to the significant difference between the calculated $K_{n\text{-}w}$. The ^{222}Rn activities are presented in function of the batch NAPL contents. The batch without NAPL shows a ^{222}Rn activity of 1991 ± 114 $Bq.m^{-3}$, similar to the production experiment (2210 ± 200 $Bq.m^{-3}$). The increase of the NAPL content in the porous media leads to the decrease of the ^{222}Rn activity reaching a value of 429 ± 24 $Bq.m^{-3}$ for θ_n = 0.2. The theoretical Rn activity calculated from Eq.1 with different NAPL contents are also presented in figure 2a (black curve). The best fit with the experimental data is obtained using a $K_{n\text{-}w}$ = 60.7 ± 6.1.

The figure 2b shows the ^{222}Rn activities for the batches containing UV-degraded diesel fuel for different NAPL contents. This set shows, like for the fresh diesel fuel, but more sharply, a decrease of the ^{222}Rn activity with the increase of the NAPL content (356 ± 63 $Bq.m^{-3}$, NAPL θ_n = 0.2). The fitted partitioning coefficient for this altered diesel fuel is $K_{n\text{-}w}$ = 74.8 ± 7.5. For the evaporated diesel (Fig. 2c), the ^{222}Rn activity also decreases, but at a lower intensity than the fresh and UV-degraded diesel. Indeed, the batch without diesel fuel shows a ^{222}Rn activity of 1413 ± 215 $Bq.m^{-3}$ which is lower than for the others because of the type of soil used for this batch, and the most NAPL saturated batch presents a ^{222}Rn activity of 547 ± 28 $Bq.m^{-3}$ (NAPL θ_n = 0.2). The partitioning coefficient is $K_{n\text{-}w}$ = 25.1 ±.2.5.

3.3.2. Partitioning coefficient (K_n) of fresh and altered gasoline

For the fresh gasoline, the porous media without NAPL shows a lower activity than the diesel fuel batch set, with a ^{222}Rn activity of 1292 ± 121 $Bq.m^{-3}$ (Fig. 3a) which is explained by the type of soil used for this batch. The increase of gasoline content in the batches lead to a decrease of the ^{222}Rn activity (389 ± 52 $Bq.m^{-3}$ for θ_n = 0.2). The fitted partitioning coefficient was also calculated and the best fit is obtained

for a $K_{n\text{-}w}$ = 37.4 ± 5.6. The UV-degraded gasoline (Fig. 3b) also shows a decrease of the ^{222}Rn activities, but to a lesser extent, reaching 658 ± 24 $Bq.m^{-3}$ (θ_n = 0.2). The partitioning coefficient between NAPL and water is $K_{n\text{-}w}$ = 33 ± 4.9. The evaporated gasoline shows a ^{222}Rn activity of 1995± 195 $Bq.m^{-3}$ (θ_n = 0) decreasing to 673 ± 70 $Bq.m^{-3}$ (θ_n = 0.2), leading to a $K_{n\text{-}w}$ of 30.8 ± 4.6. The table 1 summarizes the different $K_{n\text{-}w}$ found is this study (see SI for statistical results).

3.4. Molecular investigation of the fresh and degraded NAPLs, identification of by-products

3.4.1 Chemical composition of diesel fuel

The most volatile compounds identified using the HS-GCMS are presented in the figure 4. The fresh diesel fuel chromatogram (Fig. 4a, Table 2) is principally composed by linear n-alkanes ranging from n-C5 and n-C15 and by branched n-alkanes. Other compounds such as cyclic hydrocarbons, alkenes and BTEX are also encountered. The chromatogram corresponding to the UV treatment (Fig. 4b, Table 2) is rather similar to the fresh diesel without any total loss of compounds. However, a general decrease of the peaks intensity is observed with a TIC area representing 73 % of the fresh diesel fuel. The percentage of the different compounds in the different fractions (<C10 and >C10) confirmed the TIC area decrease, mainly in the <C10 fraction for the UV-degraded diesel fuel. The chromatogram corresponding to the evaporation treatment is different (Fig. 4c, Table 2). The first 12 minutes of the TIC is characterized by an absence of peaks, corresponding to the loss of the most volatile compounds (ranging from n-C5 and n-C8). The area of the evaporated diesel TIC represents 16% of the fresh diesel fuel. The percentage of the different compounds in the different fractions also shows a decrease in the evaporated diesel fuel mainly in the <C10 fraction.

The liquid GC-MS in scan mode permits to identify the different major hydrocarbons of moderate to low volatility present in the fresh diesel fuel (Fig. 5a, Table 2). The diesel fuel

matrix is complex and the separation of the different compounds is limited, reducing the possible identification of the different compounds. The fresh diesel fuel is principally composed by n-alkanes such as linear n-alkanes and branched n-alkanes ranging from n-C8 to n-C27. The diesel fuel is also composed by alkenes, cyclo-alkanes and BTEX. The photodegraded diesel fuel (Fig. 5b) shows a similar chromatogram pattern with the same by-products and similar intensity. The percentages of the different families in the different fractions (< C10, C10 – C15, >C15) do not show high variations for the fresh and UV-degraded diesel fuel. A slight increase of the cycloalkanes and methyl alkanes is observed in the >C15 fraction for the UV-degraded diesel fuel (Table 2). In contrary, the diesel fuel artificially evaporated (Fig. 5c) under the hood (30 % in weight) shows variations of the chromatogram compared to fresh and UV-degraded diesel fuel. The lightest fraction of the diesel fuel (until 17 min) is vaporized resulting in the absence of peaks. The percentages show high decrease of the different compounds in the different fractions, mainly in the <C10 and C10 – C15 fractions, containing in particular cyclo-alkanes.

3.4.2 Chemical composition of gasoline

The most volatized compounds are presented in the figure 6. The fresh gasoline chromatogram (Fig. 6a, Table 2) is composed by linear n-alkanes, alkenes (n-C_5 to n-C_8), branched n-alkanes, alkenes and cyclic hydrocarbons. In addition, BTEX represents a large fraction of the chromatogram, eluting between 10 and 20 min. The chromatogram corresponding to the UV treatment (Fig. 6b, Table 2) is rather similar to the fresh gasoline with similar peaks intensity in TIC area. The percentage of the different compounds in the different fractions (<C5 and >C5) also confirms the general observations with the TIC with similar percentages in the different fractions. The chromatogram corresponding to the evaporation treatment is slightly different (Fig. 6c, Table 2). Several peaks at the beginning of the chromatogram, corresponding to

alkanes and alkenes, disappeared and the area of the evaporated gasoline TIC represents 96% of the fresh gasoline. The percentage of the different compounds in the different fractions also shows a decrease in the evaporated gasoline in the <C5 fraction. The >C5 fractions reveals an increase in the different fractions, resulting from a concentration of the compounds into NAPL due to evaporation. Indeed, the evaporation results in the removal of the lower boiling compounds and a relative abundance increase of the higher boiling compounds into NAPL, leading to higher partial pressure in the gas phase (Raoult law).

The fresh gasoline (Fig. 7a, table 2) is characterized by low molecular-mass hydrocarbons mainly eluting before 10 min. Monoaromatic compounds are predominant in the sample. Alkanes (n-C_8 to n-C_{16}), alkenes, cycloalcanes and isoalkanes complete the composition. The UV-degraded gasoline (Fig. 7b, Table 2) chromatogram pattern is similar to the fresh chromatogram pattern with the predominance of low molecular-mass hydrocarbons at similar intensity. In contrast to the evaporated diesel fuel (Fig. 7c), the evaporated gasoline does not clearly show difference with the fresh gasoline. The percentage of the different compounds in the <C10 and >C10 fractions for the fresh, UV-degraded and evaporated gasoline does not show clear and logical variations (Table 2).

4. Discussion

4.1. Radon production in the porous media

Radon production can evolve in two different ways depending on soil moisture. Low soil moisture contents can lead to an increase of soil emanation (Nazaroff, 1992; Hosoda et al., 2007) in comparison with dry soil. Actually, for dry soil, a significant fraction of ^{222}Rn that escape from a grain due to recoil enters in another grain and thus does not stay in porosity, inducing low EC_{Ra} as can be seen for the first batch without water (Fig. 1). When a small amount of water is added, a higher fraction of ^{222}Rn is trapped in the porosity, leading to an increase of EC_{Ra}. This behavior is also observed in this study with the increase of EC_{Ra} for the batches with small content of water (θ_w 0.01 – 0.02) (Fig. 1). However, higher soil moisture reduces gas mobility.

Different factors influence the ^{222}Rn emanation from soils (*ie.* temperature, soil physical and chemical properties). When the temperatures are lower, the number of radon atoms adsorbed to particles increases, leading to a decrease of the ^{222}Rn activity (Baskaran, 2016). The different set of batches were carried out at different time and the room temperature changed slightly (from 25 °C to 15 °C). This temperature change could explain the variation of ^{222}Rn activity. Another explanation can come from the soil material used in this study. The soil was sampled from a pond area, close to the laboratory. A large amount of soil was necessary for the different set of batches and a hole of approximately 1.5 m deep was dug. The composition of the soil was not the same from the surface and the bottom with more fine particles encountered deeper. This soil composition variation could explain the ^{222}Rn activity variation between the batch sets. Thu et al., (2020) investigated the ^{222}Rn emanation and diffusion from soil in function of different soil compositions. They noted a dependence of the radon emanation on iron content and pH.

4.2. Molecular composition

Diesel fuel is a complex mixture of different hydrocarbons. The major compounds encountered are straight n-alkanes, isoprenoids (branched n-alkanes), cyclo-alkanes and aromatics (Christensen et al., 1987). A typical fresh diesel fuel chromatogram is characterized by a dominance of n-alkanes peaks, appearing in a regular pattern and covering all the chromatogram (Christensen et al., 1993). Gasoline fuel is obtained from the distillation and cracking of crude oil (El Naggar et al., 2017). Cracking produces, from long chain alkanes, smaller alkenes at high temperature. Typical gasoline fuel is composed by over 200 petroleum-derived chemicals (El Naggar et al., 2017) with a dominance of aromatic compounds and branched alkanes over n-alkanes.

The fresh commercial diesel fuel and gasoline used in this study, characterized with MS in scan mode using GC-MS reveals similar patterns than the ones observed in literature. On the contrary, the artificial degradations carried out in this study permit to reveal different behaviors. The different chromatographic techniques employed in this study do not permit to observe any difference concerning the UV-light degradation with the fresh material except a diminution of the area of the total chromatogram for the UV-degradation compared to the fresh diesel fuel with the HS-GCMS analyses. Garrett et al., (1998) also performed artificial weathering of Alaskan crude oil, by its exposure to UV-light, and observed no effect of the illumination on the total ion chromatograms as well. However, the use of thin layer chromatography showed variations with the conversion of the aromatics hydrocarbons to resins or polar compounds. Douglas et al., (2002) also investigated the effect of UV light on oil molecular composition using Single Ion Monitoring (SIM) mode. They showed that large polycyclic aromatic hydrocarbons are more affected by photooxidation as well as the more alkylated compounds. Further investigation of the degraded products, focusing on certain molecules could help to distinguish some variations between fresh and UV-degraded chromatograms patterns.

419 The artificial evaporation effect on the molecular composition is quite different from the
420 artificial photooxidation. In this study, the artificial diesel fuel evaporation under the hood
421 removes the compounds presenting a chromatographic retention time below 12 min, as
422 observed in liquid and head-space chromatographs (Fig 4c and 5c). Villa et al., (2010) studied
423 the effects of the evaporation on the molecular composition of diesel fuel. They showed a loss
424 of hydrocarbons with chain lengths less than 14 carbons in addition to other unsaturated and
425 cyclic hydrocarbons. Prince et al., (2003) also showed the release of the lightest compounds
426 (C4 – C18) in result to the evaporative process. As a general feature, the evaporative process
427 will start with the removal of all components with short retention times including n-alkanes and
428 isoprenoids. Sometimes, the process can lead to the evaporation of components with higher
429 retention times. However, the ratio between the n-alkanes and isoprenoids will not change
430 (Wang et al., 1990). In the present study, the gasoline chromatograms do not show any variation
431 of the composition or peak intensity between fresh and evaporated material except a removal
432 of the first peaks (first two minutes, Fig. 7c) and a relative increase of the high boiling
433 compounds in the HS-GCMS. Turner et al., (2012) also studied the effects of weathering
434 (evaporation) on the molecular composition of gasoline using liquid GCMS. They reported no
435 special variation of the chromatogram pattern between a 0% weathered sample and 50%
436 weathered sample. This could explain the absence of variation in this study with gasoline
437 subject to 50% evaporation in weight.

438 **4.3. Determination of ^{222}Rn partitioning coefficients of fresh and aged NAPLs**

439 Very little data is available concerning the radon partitioning coefficient for NAPL mixtures.
440 Hunkeler et al. (1997) measured the ^{222}Rn partitioning coefficient for an unspecified diesel fuel
441 and Schubert et al. (2007a) determined ^{222}Rn partitioning coefficient for three synthetic NAPL
442 mixtures representing gasoline, and diesel fuel (Table 3). To our knowledge, no data is currently
443 available concerning the partitioning coefficient of complex degraded NAPLs.

444 On the other side, pure NAPLs such as Benzene and Toluene radon partitioning coefficient can
445 be encountered in the literature (Clever, 1979; Abraham et al., 1994; Schubert et al., 2007a, b).
446 The table 3 gathers several coefficient partitions of pure NAPLs of interest from the literature.
447 The next paragraph is dedicated to the comparison of the different complex NAPLs mixtures
448 and pure NAPLs.
449 First of all, the results show that, in spite of a wide range covered by the radon partitioning
450 coefficients $K_{n\text{-}w}$ (26 – 75), the different commercial NAPLs investigated have a strong affinity
451 with radon. The fresh diesel fuel shows higher partitioning coefficient than fresh gasoline. For
452 both fresh NAPL used in this study, the partitioning coefficient $K_{n\text{-}w}$ are similar to those
453 presented in Schubert et al. (2007b) (60.7 ± 6.1 vs 60 ± 1.3 and 37.4 ± 5.6 vs 38.9 ± 0.9, for
454 diesel fuel and gasoline, respectively), despite the fact that this study used commercial mixture
455 while Schubert et al. (2007b) used simplified synthetic mixtures. Indeed, the gasoline used in
456 Schubert et al., (2007b) study was a laboratory made mixture composed by 50 % of iso-octane,
457 40 % of BTEX and 10 % alkene while the commercial gasoline used in this study is composed
458 by multiple compounds and especially a large proportion of BTEX. Coefficient partition of
459 several BTEX has been determined in the literature indicating intermediate $K_{n\text{-}w}$ values
460 (between 44.7 and 51.3, table 3). This could explain the lower $K_{n\text{-}w}$ encountered for gasoline.
461 The diesel fuel used in Schubert et al., (2007b) was composed at 60% by hexadecane and 15%
462 cyclohexane while the one used in this study is mainly composed by different alkanes from C8
463 to C27. One explanation for this $K_{n\text{-}w}$ similarity is that the compounds used by Schubert et al.,
464 (2007b) may drive the partitioning coefficient behavior. The main result brought by this study
465 is the variation of the partitioning coefficient (compared to fresh NAPLs) when the diesel fuel
466 is degraded. On the other hand, the gasoline did not show any significant variations related to
467 degradation, probably due to the too slight degradation (see part 4.2). The evaporation of 50%
468 in weight of the gasoline was extremely rapid. However, the chromatogram pattern does not

show large differences for the evaporation treatment. This could be due to the evaporation of an extremely volatile compound. The evaporation leads to a reduction of the diesel fuel affinity for ^{222}Rn, whereas the UV-degradation engenders higher affinity of diesel fuel for ^{222}Rn. This feature demonstrates that for diesel, the degradation processes will change the affinity of NAPLs toward ^{222}Rn compared to fresh products. The partitioning coefficients gathered in the literature (Table 3) may explain the variations of $K_{n\text{-}w}$. When a diesel fuel is artificially evaporated, the results show a removal of the lightest fraction which is composed by short alkanes chains and cycloalcanes. The $K_{n\text{-}w}$ of hexane and cyclohexanes are 58.1 and 63.3, respectively. When those molecules are removed by evaporation, a modification of the $K_{n\text{-}w}$ is then expected, as measured in this study. In addition, the hexadecane $K_{n\text{-}w}$ has also been reported with a value of 33.3 (Abraham et al., 1994).

As Schubert et al., (2007a) stated, the use of Radon method is not applicable without restrictions. Indeed, as found in this study, the partitioning coefficient evolves in relation with the NAPL alteration. This change in the partitioning coefficient will lead to incorrect interpretation of the Radon Deficit Factor. A simple calculation of the NAPL saturation (eq. 3) permits to estimate the NAPL saturation changes in relation with the $K_{n\text{-}w}$. The use of a fresh diesel fuel $K_{n\text{-}w}$ (60) instead of a $K_{n\text{-}w}$ of evaporated diesel fuel (26) in an area where diesel fuel has been exposed to air will lead to an overestimation of approximatively 50% of the NAPL saturation. In the same way, if a $K_{n\text{-}w}$ of a fresh diesel fuel is used instead of fresh gasoline, the overestimation of the NAPL saturation would be about 30%. However, semi-quantitative measurements are still operable since ^{222}Rn shows a strong affinity to NAPLs either fresh or degraded.

In this study, the different pure compounds forming the diesel fuel and gasoline present a $K_{n\text{-}w}$ ranging from 33 to 63 (fresh compounds). The fresh diesel fuel detains a $K_{n\text{-}w}$ of 60.7 and the gasoline a $K_{n\text{-}w}$ of 37. This could suggest that the $K_{n\text{-}w}$ for this kind of NAPLs mixtures should

494 reasonably ranging between 30 and 60. Despite the remaining uncertainty in the Kn of one
495 degraded NAPL, the presented results allowed to specify the full range of Rn for field NAPL.
496

5. Conclusion

This study investigates the variations of the partitioning coefficient (K_{n-w}) of different fresh commercial NAPL mixtures (diesel fuel and gasoline) and commercial NAPL mixtures degradations (evaporation and photooxidation). The results show different partitioning coefficients of the fresh diesel fuel and gasoline which are similar with previous K_{n-w} reported in the literature. The NAPL artificial degradations carried out in this study engender variations of the K_{n-w}. The evaporated diesel fuel shows lower K_{n-w} than the fresh diesel fuel whereas the UV-degraded diesel fuel shows higher K_{n-w} than fresh diesel fuel. For the gasoline, the variations of the K_{n-w} in relation with the degradation processes are more tenuous. The molecular characterization of the diesel fuel, using GCMS in scan mode, do not permit to differentiate fresh and UV-degraded products (except the diminution of the intensity concerning the HS approach). The evaporated diesel fuel chromatogram is different with the absence of peaks at the beginning of the chromatogram (first 17 min). The gasoline molecular composition is not variable between the different treatments using the GCMS method in scan mode, except a removal of the first peaks (first 2 min) in the HS approach. As previously reported in the literature, the ^{222}Rn is a good proxy parameter for soil NAPL delineation. In the calculation and modelling, the partitioning coefficient is of pivotal importance. This study emphasis the importance of the study of the K_{n-w} variability as it can lead to an false estimation of NAPL saturation. Therefore, it is extremely important to explore the effects of different parameters that could modify the K_{n-w}. This study reveals that NAPL degradation modify the partitioning coefficient in relation with the molecular composition. Future researches are thus needed to decipher the relationship between NAPL molecular composition and ^{222}Rn partitioning coefficient K_{n-w} in order to:

– better understand the evaporation intensity effects on the diesel fuel and gasoline K_{n-w}

– Investigate the microbial degradation effects on the K_{n-w}

– Investigate the effects of different degradation processes on the same NAPL mixture (evaporation coupled to photooxidation, evaporation coupled to microbial degradation).

Conflict of Interest

The authors declare that the research was conducted in the absence of any commercial or financial relationships that could be construed as a potential conflict of interest.

Acknowledgements

The authors would like to thank the financial support of the Carnot ISIFoR and IdEx for this study.

References

Abraham, M. H., Chadha, H. S., & Leo, A. J. (1994). Hydrogen bonding: XXXV. Relationship between high-performance liquid chromatography capacity factors and water-octanol partition coefficients. *Journal of Chromatography A*, *685*(2), 203-211.

Andrews, J. N., & Wood, D. F. (1972). *Mechanism of radon release in rock matrices and entry into groundwaters*. Bath University of Technology, England.

Auria, M., Emanuele, L., Racioppi, R., & Velluzzi, V. (2008). Photochemical degradation of crude oil: Comparison between direct irradiation, photocatalysis, and photocatalysis on zeolite. *Journal of Hazardous Materials*, *164*(1), 32-38.

Barrio-Parra, F., Izquierdo-Díaz, M., Díaz-Curiel, J., & De Miguel, E. (2021). Field performance of the radon-deficit technique to detect and delineate a complex DNAPL accumulation in a multi-layer soil profile. *Environmental Pollution*, *269*, 116200.

Baskaran, M. (2016). *Radon: A tracer for geological, geophysical and geochemical studies* (Vol. 367). Springer, Basel:.

Brusseau, M. L., Nelson, N. T., & Costanza-Robinson, M. S. (2003). Partitioning tracer tests for characterizing immiscible-fluid saturations and interfacial areas in the vadose zone. *Vadose Zone Journal*, *2*(2), 138-147.

Castelluccio, M., Agrahari, S., De Simone, G., Pompilj, F., Lucchetti, C., Sengupta, D., ... & Tuccimei, P. (2018). Using a multi-method approach based on soil radon deficit, resistivity, and induced polarization measurements to monitor non-aqueous phase liquid contamination in two study areas in Italy and India. *Environmental Science and Pollution Research*, *25*(13), 12515-12527.

Chitra, N., Danalakshmi, B., Supriya, D., Vijayalakshmi, I., Sundar, S. B., Sivasubramanian, K., & Jose, M. T. (2018). Study of Radon and Thoron exhalation from soil samples of different grain sizes. *Applied Radiation and Isotopes*, *133*, 75-80.

Christensen, L. B., Arvin, E., & Jensen, B. (1987). Solubility of Oil products in groundwater. In *Rep. to Dan. Environ. Agency*. Dep. Environ. Eng., Tech. Univ. of Denmark Lyngby.

Christensen, L. B., & Larsen, T. H. (1993). Method for determining the age of diesel oil spills in the soil. *Groundwater Monitoring & Remediation*, *13*(4), 142-149.

Clever, H. L. (1979). Krypton, Xenon and Radon, International Union of Pure and Applied Chemistry, Solubility Data Series, VoL. 2, Pergamon Press, Oxford.

Cohen, G. J., Bernachot, I., Su, D., Höhener, P., Mayer, K. U., & Atteia, O. (2019). Laboratory-scale experimental and modelling investigations of 222Rn profiles in chemically heterogeneous LNAPL contaminated vadose zones. *Science of the Total Environment*, *681*, 456-466.

Cohen, R., & Mercer, J. (1993). DNAPL Site Evaluation, EPA 600/R-93/022. Office of Research and Development, U.S. EPA.

Ćujić, M., Mandić, L. J., Petrović, J., Dragović, R., Đorđević, M., Đokić, M., & Dragović, S. (2020). Radon-222: environmental behavior and impact to (human and non-human) biota. *International Journal of Biometeorology*, 1-15.

Davis, C., Cort, T., Dai, D., Illangasekare, T. H., & Munakata-Marr, J. (2003). Effects of heterogeneity and experimental scale on the biodegradation of diesel. *Biodegradation*, *14*(6), 373-384.

Deeds, N. E., Pope, G. A., & McKinney, D. C. (1999). Vadose zone characterization at a contaminated field site using partitioning interwell tracer technology. *Environmental Science & Technology*, *33*(16), 2745-2751.

DeWayne-Cecil, L. D., & Green, J. R. (1999). Radon-222 as a tracer in the hydrogeologic environment. In: Cook, P, Herczeg, A. (eds), *Isotopes in Subsurface Hydrology*, Kluwer, Buston *Chapter 6, pp 175-195*.

Douglas, G. S., Owens, E. H., Hardenstine, J., & Prince, R. C. (2002). The OSSA II pipeline oil spill: the character and weathering of the spilled oil. *Spill Science & Technology Bulletin*, *7*(3-4), 135-148.

Dwarakanath, V., Deeds, N., & Pope, G. A. (1999). Analysis of partitioning interwell tracer tests. *Environmental science & technology*, *33*(21), 3829-3836.

Feenstra, S., & Cherry, J. A. (1996). Diagnosis and assessment of DNAPL sites. *Subsurface. In Dense Chlorinated Solvents and other DNAPLs. In: Pankow J.F., Cherry J. A.,Groundwater: History, Behavior, and Remediation*, Waterloo Press, Portland, Oregon, 395-465.

Fernández, J., Arjol, M. A., & Cacho, C. (2013). POP-contaminated sites from HCH production in Sabiñánigo, Spain. *Environmental Science and Pollution Research*, *20*(4), 1937-1950.

Galhardi, J. A., & Bonotto, D. M. (2012). Radon in groundwater contaminated by dissolved hydrocarbons in Santa Bárbara d´ Oeste, São Paulo State, Brazil. *Applied Radiation and Isotopes*, *70*(10), 2507-2515.

García-González, J. E., Ortega, M. F., Chacón, E., Mazadiego, L. F., & De Miguel, E. (2008). Field validation of radon monitoring as a screening methodology for NAPL-contaminated sites. *Applied Geochemistry*, *23*(9), 2753-2758.

Garrett, R. M., Pickering, I. J., Haith, C. E., & Prince, R. C. (1998). Photooxidation of crude oils. *Environmental Science & Technology*, *32*(23), 3719-3723.

Höhener, P., & Surbeck, H. (2004). Radon-222 as a tracer for nonaqueous phase liquid in the vadose zone: Experiments and analytical model. *Vadose Zone Journal*, *3*(4), 1276-1285.

Horiuchi, K., & Murakami, Y. (1981). A new procedure for the determination of radium in water by extraction of radon and application of integral counting with a liquid scintillation counter. *The International Journal of Applied Radiation and Isotopes*, *32*(5), 291-294.

Hosoda, M., Shimo, M., Sugino, M., Furukawa, M., & Fukushi, M. (2007). Effect of soil moisture content on radon and thoron exhalation. *Journal of Nuclear Science and Technology*, *44*(4), 664-672.

Hunkeler, D., Hoehn, E., Höhener, P., & Zeyer, J. (1997). Rn-222 as a partitioning tracer to detest diesel fuel contamination in aquifers: laboratory study and field observations. *Environmental Science and Technology, 31*, 3180–3187. https://doi.org/10.1021/es970163w.

Jho, E. H., Ryu, H., Shin, D., Kim, Y. J., Choi, Y. J., & Nam, K. (2014). Prediction of landfarming period using degradation kinetics of petroleum hydrocarbons: test with artificially contaminated and field-aged soils and commercially available bacterial cultures. *Journal of Soils and Sediments*, *14*(1), 138-145.

Mariner, P. E., Jin, M., Studer, J. E., & Pope, G. A. (1999). The first vadose zone partitioning interwell tracer test for nonaqueous phase liquid and water residual. *Environmental Science & Technology*, *33*(16), 2825-2828.

Mason, B.H., & Moore, C.B. (1982). *Principles of geochemistry* (Vol. 74, No. 3, p. 262). Wiley, New York.

Naggar, A.E., Elkhateeb, A., Altalhi, T.A., El Nady, M.M., Alhadhrami, A., Ebiad, M.A., ... & Elhardallou, S.B. (2017). Hydrocarbon compositions and physicochemical characteristics for the determination of gasoline quality: An implication from gas chromatographic fingerprints. *Energy Sources, Part A: Recovery, Utilization, and Environmental Effects*, *39*(15), 1694-1699.

Nazaroff, W. W. (1992). Radon transport from soil to air. *Reviews of Geophysics*, *30*(2), 137-160.

N. Nelson, M. Oostrom, T. W. Wietsma & M. L. Brusseau, 1999.Partitioning tracer method for the in situ measurement of DNAPL saturation: influence of heterogeneity and sampling method. Environmental Science and Technology, 33, 4046-53.

Prince, R. C., Garrett, R. M., Bare, R. E., Grossman, M. J., Townsend, T., Suflita, J. M., ... & Lindstrom, J. E. (2003). The roles of photooxidation and biodegradation in long-term weathering of crude and heavy fuel oils. *Spill Science & Technology Bulletin*, *8*(2), 145-156.

Robbins, G. A., Deyo, B. G., Temple, M. R., Stuart, J. D., & Lacy, M. J. (1990). Soil-Gas Surveying for Subsurface Gasoline Contamination Using Total Organic Vapor Detection Instruments Part I. Theory and Laboratory Experimentation. *Groundwater Monitoring & Remediation*, *10*(3), 122-131.

Rodier, J., Legube, B., Merlet, N., & Brunet, R., 2009. L'analyse de l'eau-9e éd.: Eaux naturelles, eaux résiduaires, eau de mer. Dunod.

Safarova, V. I., Sapelnikova, S. V., Djazhenko, E. V., Teplova, G. I., Shajdulina, G. F., & Kudasheva, F. K. (2004). Gas chromatography–mass spectrometry with headspace for the analysis of volatile organic compounds in waste water. *Journal of Chromatography B*, *800*(1-2), 325-330.

Sakoda, A., Ishimori, Y., & Yamaoka, K. (2011). A comprehensive review of radon emanation measurements for mineral, rock, soil, mill tailing and fly ash. *Applied Radiation and Isotopes*, *69*(10), 1422-1435.

Schubert, M. (2015). Using radon as environmental tracer for the assessment of subsurface Non-Aqueous Phase Liquid (NAPL) contamination–A review. *The European Physical Journal Special Topics*, *224*(4), 717-730.

Schubert, M., Freyer, K., Treutler, H. C., & Weiss, H. (2002). Using radon-222 in soil gas as an indicator of subsurface contamination by non-aqueous phase-liquids (NAPLs). *Geofísica Internacional*, *41*(4), 433-437.

Schubert, M., Lehmann, K., & Paschke, A. (2007b). Determination of radon partition coefficients between water and organic liquids and their utilization for the assessment of subsurface NAPL contamination. *Science of the Total Environment*, *376*(1-3), 306-316.

Schubert, M., Paschke, A., Lau, S., Geyer, W., & Knöller, K. (2007a). Radon as a naturally occurring tracer for the assessment of residual NAPL contamination of aquifers. *Environmental Pollution*, *145*(3), 920-927.

Schubert, M., Pena, P., Balcazar, M., Meissner, R., Lopez, A., & Flores, J. H. (2005). Determination of radon distribution patterns in the upper soil as a tool for the localization of subsurface NAPL contamination. *Radiation Measurements*, *40*(2-6), 633-637.

Semprini, L., Hopkins, O. S., & Tasker, B. R. (2000). Laboratory, field and modeling studies of radon-222 as a natural tracer for monitoring NAPL contamination.Transport in Porous Media, 38, 223-240.

Thu, H. N. P., & Van Thang, N. (2020). The effects of some soil characteristics on radon emanation and diffusion. *Journal of Environmental Radioactivity*, *216*, 106189.

Turner, D. A., & Goodpaster, J. V. (2012). Comparing the effects of weathering and microbial degradation on gasoline using principal components analysis. *Journal of Forensic Sciences*, *57*(1), 64-69.

Villa, R.D., Trovó, A.G., & Nogueira, R.F.P. (2010). Diesel degradation in soil by Fenton process. *Journal of the Brazilian Chemical Society*, *21*(6), 1089-1095.

Wang, X., Yu, X., & Bartha, R. (1990). Effect of bioremediation on polycyclic aromatic hydrocarbon residues in soil. *Environmental Science & Technology*, *24*(7), 1086-1089.

Werner, D., & Höhener, P. (2002). Diffusive partitioning tracer test for nonaqueous phase liquid (NAPL) detection in the vadose zone. *Environmental Science & Technology*, *36*(7), 1592-1599.

Wiedemeier, T. H., Rifai, H. S., Newell, C. J., & Wilson, J. T. (1999). *Natural attenuation of fuels and chlorinated solvents in the subsurface*. Wiley, New York.

Wilson, S. C., Alcock, R. E., Sewart, A. P., & Jones, K. C. (1997). Persistence of Organic Contaminants in Sewage Sludge-Amended Soil: A Field Experiment. *Journal of Environmental Quality*, *26*(6), 1467-1477.

Wong, C. S., Chin, Y. P., & Gschwend, P. M. (1992). Sorption of radon-222 to natural sediments. *Geochimica et Cosmochimica Acta*, *56*(11), 3923-3932.

Yoon, Y. Y., Koh, D. C., Lee, K. Y., Cho, S. Y., Yang, J. H., & Lee, K. K. (2013). Using 222Rn as a naturally occurring tracer to estimate NAPL contamination in an aquifer. *Applied Radiation and Isotopes*, *81*, 233-237.

Zhang, Q., Davis, L.C., & Erickson, L.E. (1998). Effect of vegetation on transport

of groundwater and nonaqueous phase liquid contaminants. Journal of Hazard Substance Research 1, 8–20.

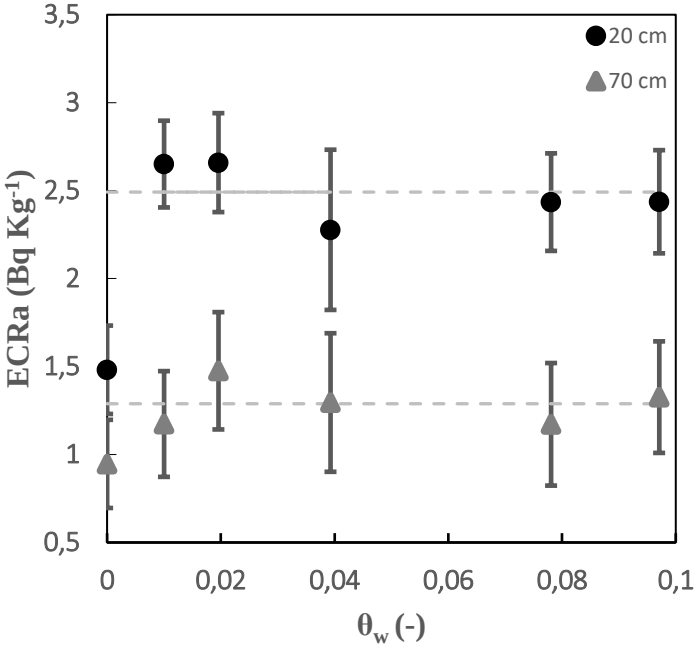

Fig. 1. ^{222}Rn production (EC_{Ra}) for the soil used in this study in relation with the water content (θ_w). Grey dashed line corresponding to ECRa mean (dry sample not included).

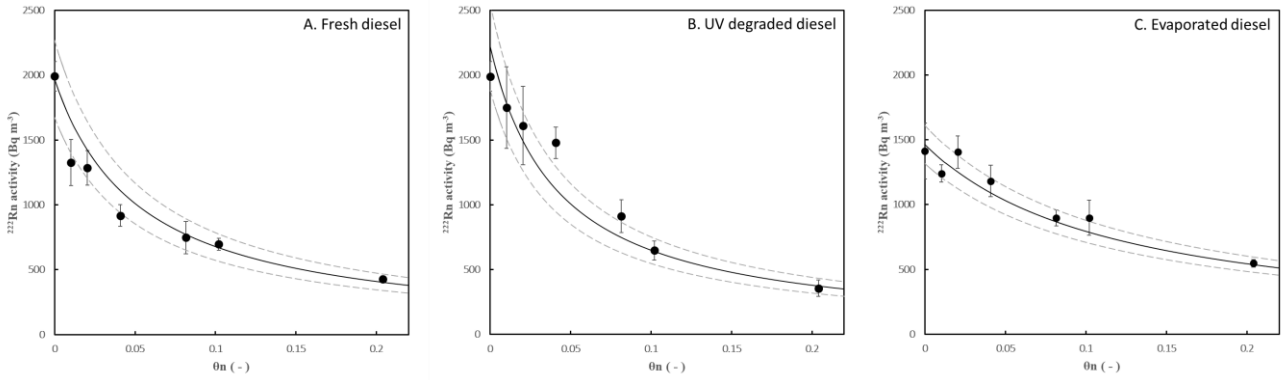

Fig. 2 Experimental (black dots) and theoretical (black curve) ^{222}Rn activity ($Bq.m^{-3}$) for (a) Fresh diesel fuel, (b) UV-degraded diesel fuel and, (c) evaporated diesel fuel as a function of the NAPL content (θ_n). Dotted lines represent errors of 15% in the gas-diesel partitioning-coefficient.

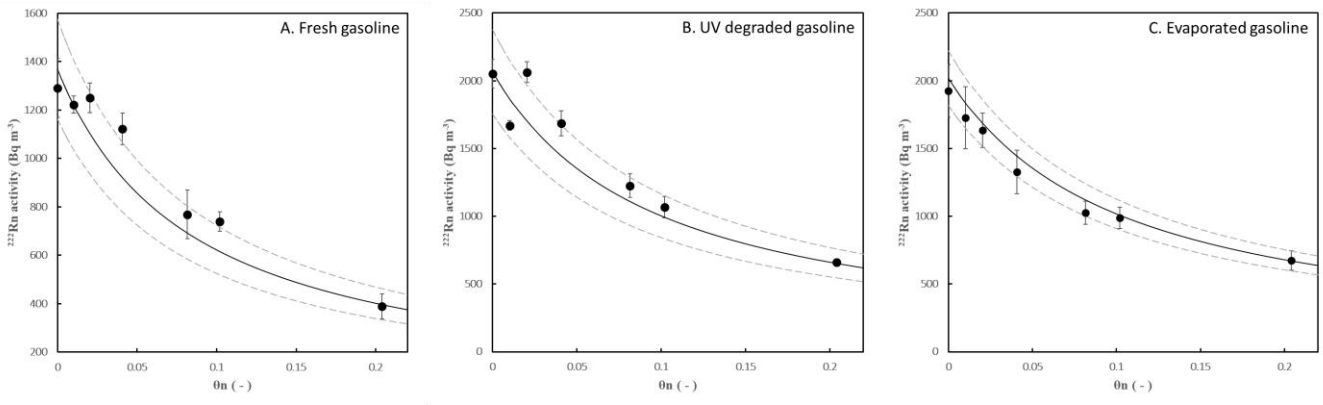

Fig. 3 Experimental (black dots) and theoretical (black curve) ^{222}Rn activity (Bq m^{-3}) for (a) Fresh gasoline, (b) UV-degraded gasoline, (c) evaporated gasoline and, (d) on site NAPL as a function of the NAPL content (θ_n). Dotted lines represent errors of 15% in the gas-gasoline partitioning-coefficient.

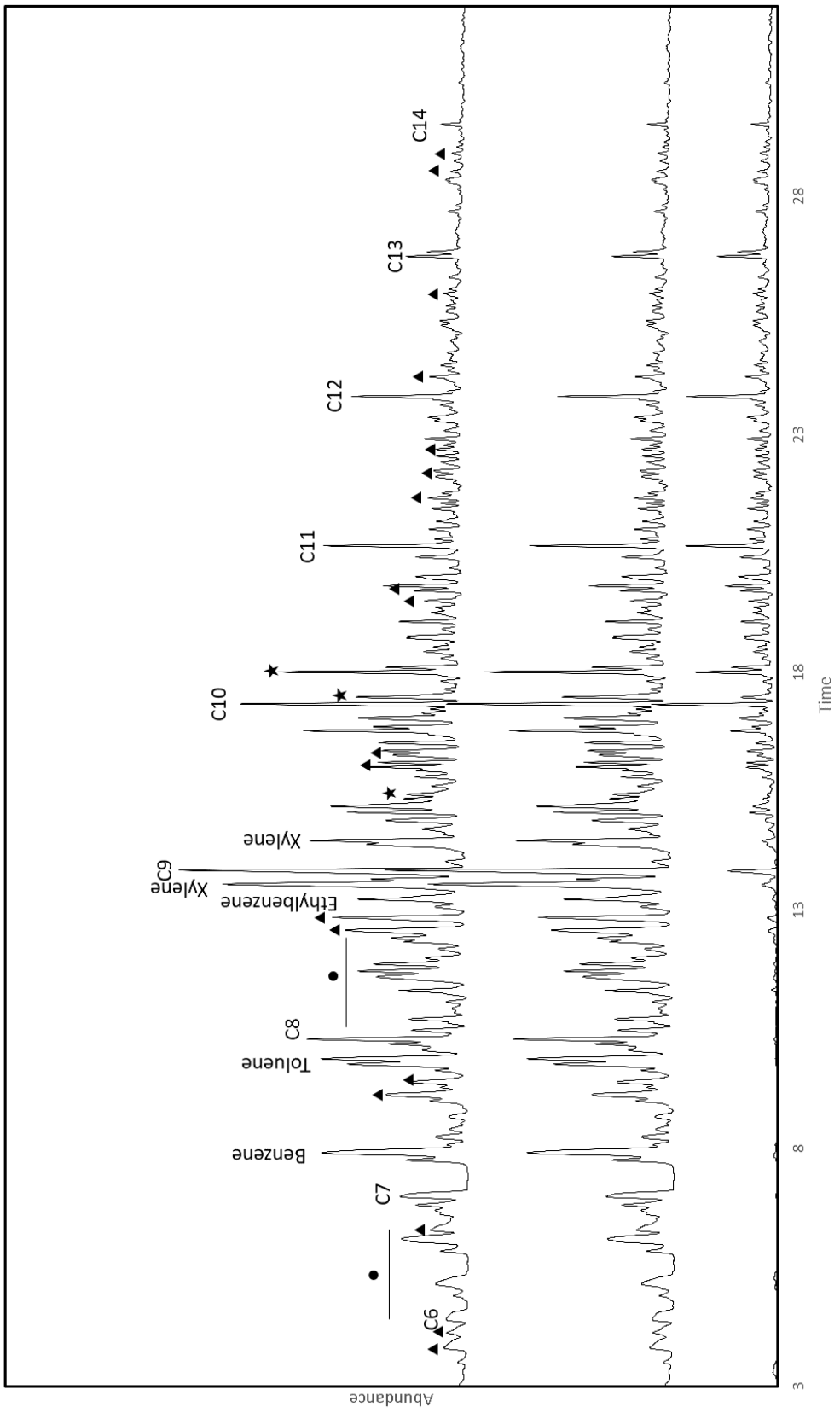

779

780 *Fig. 4 Head-Space GC-MS in scan mode chromatograms of the (a) fresh diesel, (b) UV-degraded diesel and, (c)*
781 *evaporated diesel. The C_5 to C_{15} correspond to the linear n-alkanes, triangle refers to ramified alkanes, circles*
782 *refer to cycloalkanes, stars correspond to BTEX.*

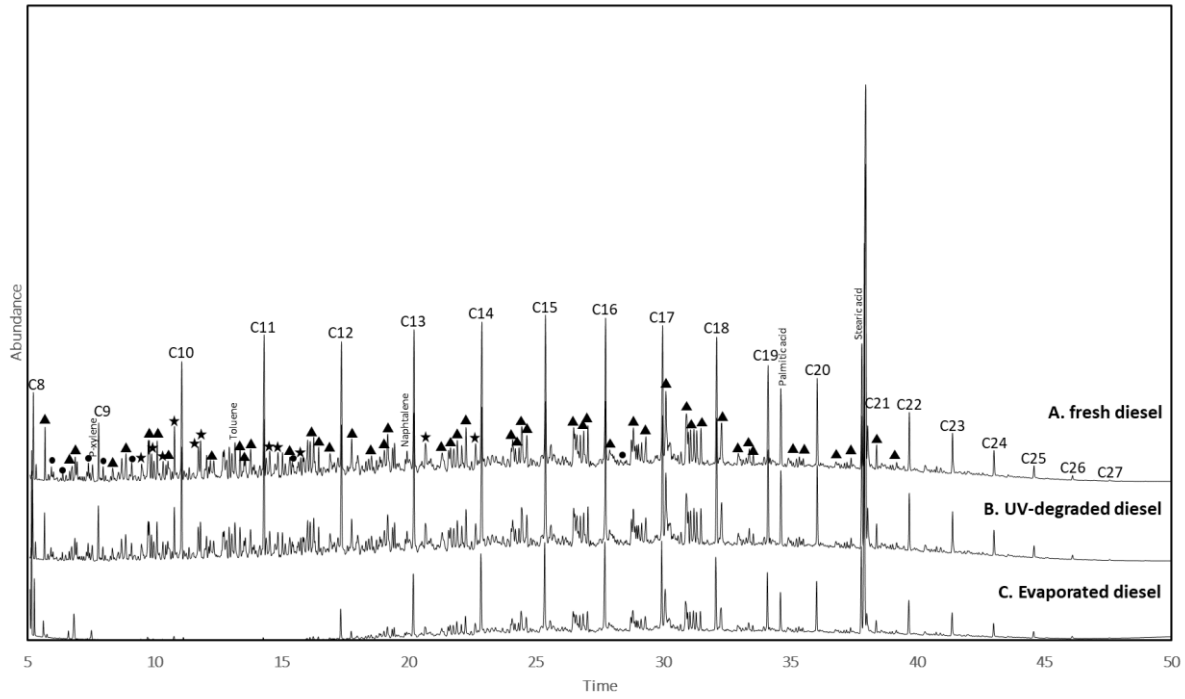

Fig. 5 Liquid GC-MS in scan mode chromatograms of the (a) fresh diesel, (b) UV-degraded diesel and, (c) evaporated diesel. The C_8 to C_{27} corresponds to the linear n-alkanes, triangle refers to ramified alkanes, circle refers to cycloalkanes, stars correspond to BTEX.

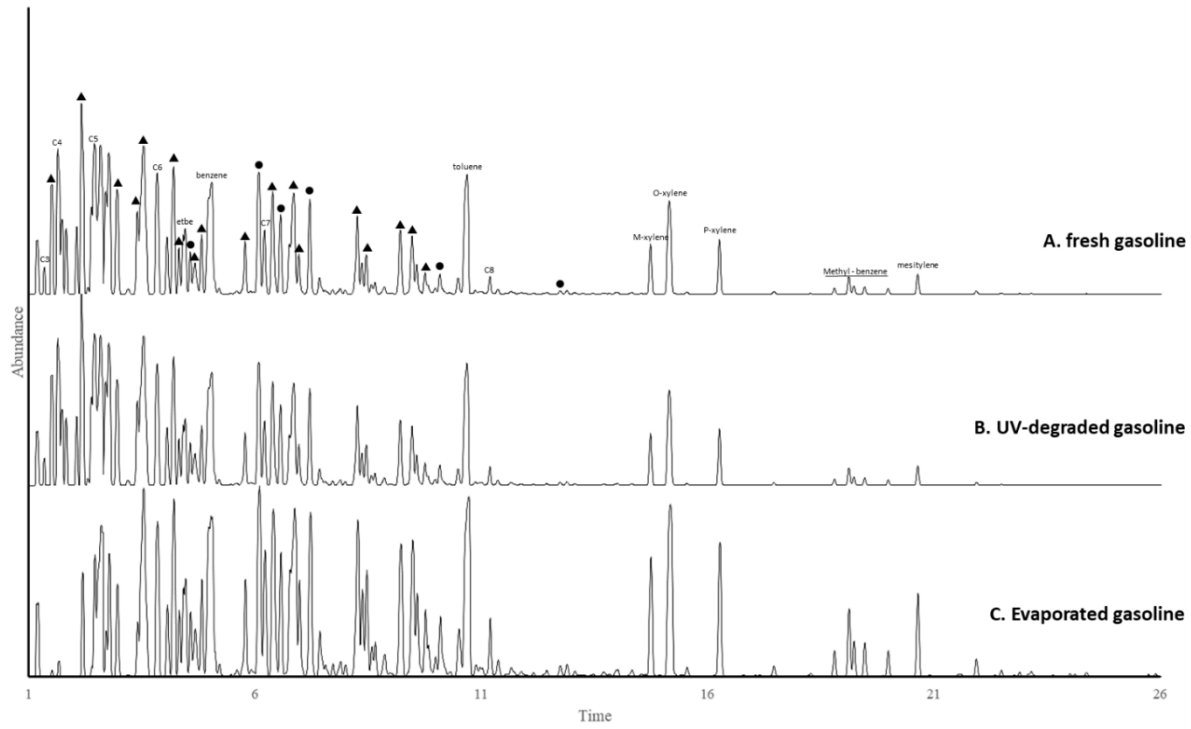

Fig. 6 Head-Space GC-MS in scan mode chromatograms of the (a) fresh gasoline, (b) UV-degraded gasoline and, (c) evaporated gasoline. The C_4 to C_8 correspond to the linear n-alkanes, triangle refers to ramified alkanes, circle refers to cycloalkanes.

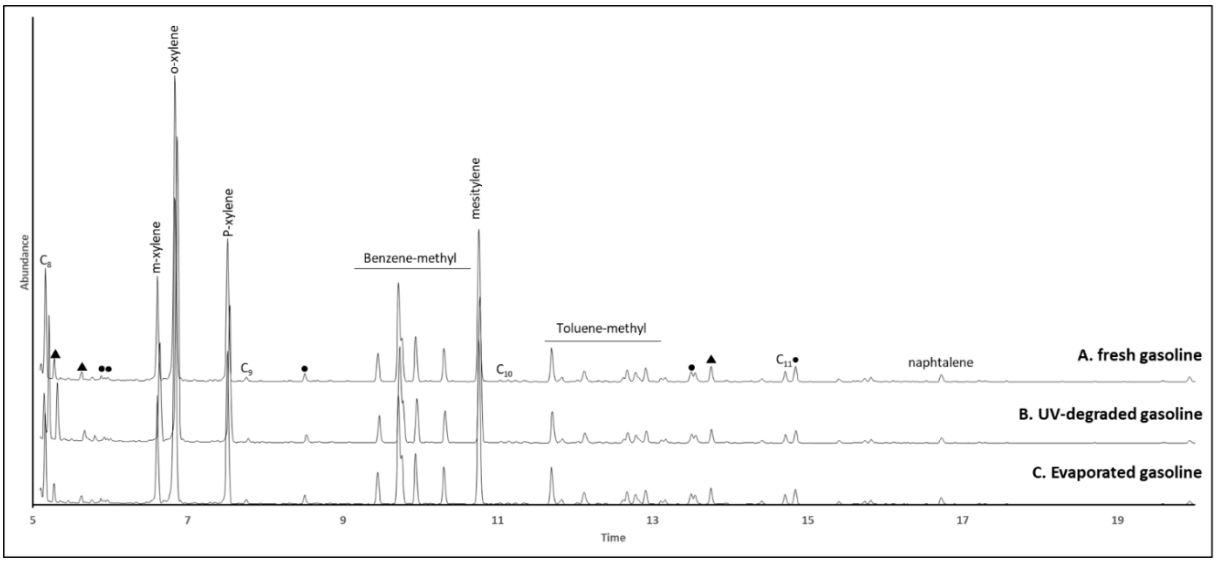

Fig. 7 Liquid GC-MS in scan mode chromatograms of the (a) fresh gasoline, (b) UV-degraded gasoline and, (c) evaporated gasoline. The C_4 to C_{10} correspond to the linear n-alkanes, triangle refers to ramified alkanes, circle refers to cycloalkanes.

	Diesel fuel	Gasoline
Fresh	60.7 ± 6.1	37.4 ± 5.6
UV-degraded	74.8 ± 7.5	33 ± 4.9
Evaporated	25.1 ± 2.5	30.8 ± 4.6

Table 1. NAPL-water partitioning coefficient for the fresh and altered diesel fuel and gasoline.

		Fresh D	UV D	Evaporated D	Fresh G	UV G	Evaporated G
Liquid GCMS	< n-C10	4.38	4.38	0.61	6.38	2.29	7.05
	cyclo < n-C10	1.27	1.27	0.00	0.79	0.29	1.14
	BTEX < n-C10	4.55	4.64	0.30	73.45	68.34	95.30
	methyl < n-C10	3.39	3.50	0.00	0.88	0.72	1.24
	n-C10-C15	14.76	15.01	1.61	0.40	0.07	0.10
	cyclo n-C10-C15	0.40	0.43	0.00	0.00	0.00	0.00
	BTEX n-C10-C15	6.90	6.89	0.21	16.61	12.66	16.85
	methyl n-C10-C15	14.53	14.33	1.12	1.50	0.67	1.02
	>C15	15.11	16.09	2.46			
	cyclo > n-C15	0.27	0.50	0.07			
	BTEX > n-C15	0.00	0.00	0.00			
	metheyl > n-C15	15.02	16.78	2.49			
HS GCMS	< n-C10	20.92	12.95	1.82	13.30	13.51	2.12
	cyclo < n-C10	26.20	17.79	0.79	7.69	7.77	1.52
	BTEX < n-C10	17.11	13.86	1.72	0.00	0.00	0.00
	methyl < n-C10	18.35	13.14	1.37	0.00	0.00	0.00
	> n-C10	3.88	3.65	2.76	20.42	20.62	17.32
	cyclo > n-C10	2.51	1.98	1.47	29.36	29.53	38.35
	BTEX > n-C10	7.07	6.38	3.49	7.12	7.60	11.67
	methyl >n-C10	3.80	3.36	2.50	13.78	13.99	23.54

Table 2. Proportion (%) of the different families (linear alkanes, ramified alkanes, monoaromatics, cycloalkanes) in the different chromatograms.

Compound	$K_{NAPL\text{-}water}$ measured	Temperature of experiment (°C)
n-hexane	58.1*	23°C
n-hexadecane	33.1"	
cyclohexane	63.3*	23°C
benzene	44.9*	23°C
toluene	51.3*	23°C
o-xylene	44.7*	23°C
Ethanol	27.9°	23°C
Diesel	60°	23°C
Diesel	40'	12°C
Gasoline	38.9°	23°C

Table 3. Coefficient partitions of several pure NAPLs from the literature (Schubert et al. (2007b); °Schubert et al. (2007a); "Abraham et al. (1994); ' Hunkeler et al. (1997)).*

Effect of NAPL mixture and alteration on ^{222}Rn partitioning coefficients: implications for NAPL subsurface contamination quantification

Le Meur Mathieu[a], Cohen Grégory[a], Laurent Mélissa[a], Höhener Patrick[b], Atteia Olivier[a]

[a] EA 4592 G&E, Bordeaux INP - Université Bordeaux Montaigne - Carnot ISIFoR, 1 allée F. Daguin, 33607 Pessac, France

[b]Aix-Marseille Université - CNRS, Laboratoire Chimie Environnement UMR 7376, 3 place Victor Hugo, 13331 Marseille, France

Supplementary information

This supplementary material presents the statistical results permitting to indicate that the Kn-w calculated from the equation 1 in the paper are significantly different. To test the significant differences between the groups, ANCOVA was used. For the ANCOVA, NAPL content (θ) was treated as fixed factors and the activity as the covariates. Statistical tests were performed using the software Xcel Stat (version 2021.1) with the significant level set at 0.05. All the variables were normalized by 1/A transformation prior to analysis.

Step 1: linear approximation of the equation : $A = \frac{1}{\left(1+\frac{\theta_w}{K_H\theta_g}+\frac{K_n\theta_n}{\theta_g}\right)} \frac{m_s}{V_g} EC_{Ra}$

The linear approximation is: $$\frac{1}{A} = \frac{(1+\theta_{w/Kh}\theta_{g)}V_g}{(ms\ EC_{Ra}\ )} + \frac{K_n V_g}{m_s\,\theta_g E C_{Ra}} * \theta_n$$

Table 1. statistical results for NAPLs and 1/A activities (R squared = 0.997, Ajusted R squared = 0.993)

Source	DF	Sum of squares	Mean squares	F	sig
Model	3	0.031	0.010	288.819	**0.000**
Error	3	0.000	0.000		
Corrected Total	6	0.031			

We found a significant linear regression between the NAPL content and the fresh diesel ($F = 3.72$; $p < 0.05$). However, the NAPL did not show significant linear regression between UV degraded diesel fuel and evaporated diesel fuel ($F = 2.45$ $p > 0.05$; $F = -0.20$ $p > 0.05$). We can state that the different 1/A of the diesel are significantly different.

Table 2. statistical results for NAPLs and 1/A activities (R squared = 0.997, Ajusted R squared = 0.994)

Source	DF	Sum of squares	Mean squares	F	Pr > F
Model	3	0.031	0.010	327.309	**0.000**
Error	3	0.000	0.000		
Corrected Total	6	0.031			

We found a significant linear regression between the NAPL content and the evaporated gasoline ($F = 4.96$; $p < 0.05$). However, the NAPL did not show significant linear regression between UV degraded gasoline and fresh gasoline ($F = 0.49$ $p > 0.05$; $F = 0.55$ $p > 0.05$). We can state that the different 1/A of the diesel are significantly different.